

EXPERIMENTAL VERIFICATION OF THE G-H MEASUREMENT MODEL BY
ULTRASONIC DIFFRACTION IN SINGLE CRYSTALS, AND NEW [110]
LONGITUDINAL PROPAGATION RESULTS

Emmanuel P. Papadakis and Frank Margetan

Center for Nondestructive Evaluation
Iowa State University
Ames, Iowa 50011

Byron P. Newberry

Department of Aerospace Engineering
University of Cincinnati
Cincinnati, OH 45221

INTRODUCTION

A calculation of diffraction loss versus normalized (dimensionless) distance is needed to correct ultrasonic attenuation measurements for beam spreading and arrive at the intrinsic material attenuation as a function of frequency.

Prior to this paper, the diffraction loss from circular piston transducers had been calculated for liquids, for isotropic solids, and for certain directions in solids with crystalline symmetry, namely along axes of 3-fold, 4-fold, and 6-fold symmetry. In the previous computerized numerical integration methods, the symmetries more complex than parabolas of revolution could not be handled because of the complexities of the slowness surfaces which made the Poynting vector, the propagation vector, and the normal to the transducer face non-coplanar.

Recently, a method has been developed which overcomes the above difficulties. The method utilizes an angular spectrum of plane waves to represent the field of the piston transducer. Through the use of small-angle approximations, this integral representation is reduced to a Gauss-Hermite series. This formulation allows for the wave propagation through anisotropic media in all directions, and can be used to study diffraction in crystals.

In this work, the model was specialized to a medium with the symmetry of interest. This specialization then permitted the diffraction loss to be calculated. Comparison of these calculations with previous theories and experiments provides a critical method for verifying the present theory.

In this paper the results on isotropic materials and on the [100] and [111] directions in silicon will be reported first and compared with previous theory and experiment to verify the performance of the

measurement model. Second, the new results on the [110] direction in silicon, germanium, and sodium chloride will be presented and compared with published experimental data.

THEORY

A. Previous Work

Previous theoretical calculations by one author⁽¹⁻³⁾ were carried on by direct computerized numerical integration of the Rayleigh integral with the spatial term $\vec{\beta} \cdot \vec{r}$ in the phase written to account for anisotropy in a direction in which the slowness surface is a paraboloid of revolution. The deviation angle between the Poynting vector \vec{P} and the propagation vector $\vec{\beta}$ of the wave carrying energy from the element of area to the field point⁽⁴⁾ is d_p , while the angle between $\vec{\beta}$ and the transducer normal \vec{n} is θ . In the theoretical work of Waterman⁽⁵⁾, the velocity v , the magnitude of the propagation vector β , and the deviation angle d_p are related by

$$v = v_0(1 - b\theta^2), \quad (1)$$

$$\beta = \beta_0(1 + b\theta^2), \quad (2)$$

$$d_p = (2B_w)^{1/2}\theta, \quad (3)$$

and

$$B_w = 2b^2 \quad (4)$$

for axes of 3-fold, 4-fold, and six-fold symmetry. (Here the subscript "w" has been appended to B_w to indicate Waterman's formulation, as the notation "B" is used in another necessary reference.) Terms in θ^3 and θ^4 are dropped. For these directions, there is no linear term, and the three vectors \vec{P} , $\vec{\beta}$, and \vec{n} are coplanar.

After the field (pressure and phase) was found from a piston source many wavelengths in diameter, the field was integrated at various distances over the face of a coaxial receiving transducer of the same diameter to find the output sensed by the receiver and hence to find the loss caused by beam spreading (ultrasonic diffraction). Computed results⁽³⁾ showed agreement between theory and experiment in predicting the shape and approximate magnitude of the diffraction loss versus normalized distance S ,

$$S = z\lambda/a^2 \quad (5)$$

where z = actual propagation distance, a = transducer radius, and λ = wavelength. In particular, both theory and experiment showed a loss peak just before a broad local minimum in the loss signifying the beginning of the far field. The position S_A of this loss peak called Peak A was predicted exactly by theory. Ultrasonic diffraction loss was measured with a pulse-echo system using essentially monochromatic rf bursts. Specimens had plane parallel faces and were interrogated by unbacked x-cut quartz transducers directly bonded to one face.

The theory of Waterman⁽⁵⁾ expressed the slowness surface (function for the magnitude β) in other directions, but these were not computed previously owing to geometrical difficulties. Specifically, the vectors \vec{P} , $\vec{\beta}$, and \vec{n} are not coplanar in more complicated directions, and the representation of β is not a paraboloid of revolution. In particular, in the [110] direction the function is a saddle surface changing sign at azimuthal increments of 90° . It is still quadratic, however, lacking a linear term.

B. New Theory

The new theory of Newberry and Thompson⁽⁶⁾ can handle the saddle surface case and, indeed, can handle a saddle surface biased by a sloping plane in an arbitrary direction. Thus, to the order of dropping terms in θ^3 and higher, the Newberry and Thompson theory can handle longitudinal wave propagation in any direction in a crystal.

The Newberry-Thompson theory expresses the wave disturbance at the face of the transducer as a Gauss-Hermite series, taking into account the transducer shape and the amplitude and phase distribution on the face of the transducer. The Gauss-Hermite method uses a particular complete set of functions to represent the angular spectrum of plane waves contained in the beam, making the approximation that the response is dominated by wave directions near the central ray of the beam. It is possible to represent a Gaussian source (peaked at the center), a piston source (as used in this paper), and anything in between. The paraxial approximation necessitates the dropping of terms higher than θ^2 .

The Newberry-Thompson theory allows for the propagation medium to have any symmetry, and represents the slowness surface as a function of angle θ of deviation from the transducer normal and as a function of angle ϕ of azimuthal about the transducer normal. The function written in terms of the components of the wave vector is

$$k/\omega = S_0 + A(k_x/\omega) + B(k_y/\omega) + C(k_x/\omega)^2 + D(k_x/\omega)(k_y/\omega) + E(k_y/\omega)^2 \quad (6)$$

The initial term S_0 is the reciprocal of the velocity v_0 along the transducer normal (z-direction) while the coefficients A, B, C, D, and E represent the slope and curvature of the slowness surface about the transducer axis. For isotropy, all are zero. For axes of 3-, 4-, and 6-fold symmetry it can be shown that

$$C = E = v_0 b \quad (7)$$

with b from Waterman's formulation, Eqs. (1) - (4), and the others are zero ($A = B = D = 0$).

For a [110]-type direction in a cubic crystal, A, C, and D are zero while C and E are the expressions for the coefficients of θ^2 given by Waterman at the two extrema, namely $\phi = 0$ and 90° . Waterman's formula is

$$b(\phi) = \frac{K_1[(2K_3 + 1)\cos^2\phi + (2K_4 - 5)\sin^2\phi]}{2(c_{11} + c_{12} + 2c_{44})} \quad (8)$$

where

$$K_1 = c_{11} - c_{12} - 2c_{44} \quad (9)$$

$$K_3 = K_1/(c_{12} + c_{44}) + 3/2 \quad (10)$$

$$K_4 = K_1/(c_{11} + c_{12}) + 3/2 \quad (11)$$

and

$$v_0 = [(c_{11} + c_{12} + 2c_{44})/2\rho]^{1/2} \quad (12)$$

so that

$$C = -\frac{v_0 K_1 (2K_3 + 1)}{2(c_{11} + c_{12} + 2c_{44})} \quad (13)$$

and

$$E = -\frac{v_o K_1 (2K_4 - 5)}{2(c_{11} + c_{12} + 2c_{44})} \quad (14)$$

The Newberry-Thompson theory goes further in a practical vein by allowing the wave to impinge upon a curved boundary of arbitrary smooth shape, to be refracted into a second medium, and to continue in that medium to impinge upon a reflector. The second medium may also be a crystal of arbitrary symmetry and orientation. In the second medium, various scans may be performed by means of moving the transducer in (on) the first medium. The operation of the Newberry-Thompson measurement model is shown diagrammatically in Fig. 1.

COMPUTATIONS

A. Verification of the Newberry-Thompson Theory

1. Method

The calculation of diffraction loss and the comparison of the calculations with both experiments and previous theories provides an opportunity for a critical check of the Newberry-Thompson theory.

For this verification, the Newberry-Thompson theory was specialized as in Fig. 2 which is to be compared with Fig. 1. Items of specialization were as follows:

- (1) The first medium was given a thickness of zero (0.0) and the "boundary" between medium 1 and medium 2 was made flat in the plane of the transducer face.

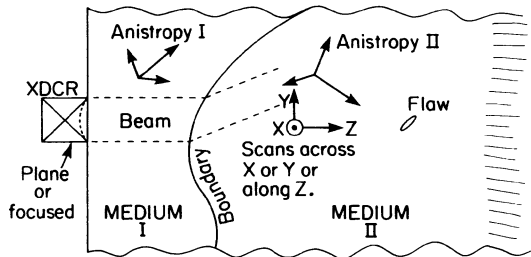


Figure 1 A diagram showing the operation of the Newberry-Thompson measurement model with its versatile capabilities.

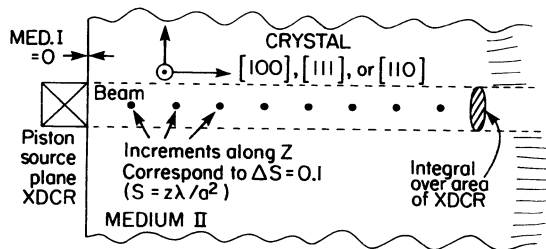


Figure 2 A diagram showing the specialization of the Newberry-Thompson measurement model to the study of diffraction loss and phase change in anisotropic materials.

(2) The transducer was specified as a circular longitudinal piston source.

(3) The propagation direction in the crystal specimen of interest was made parallel to the transducer normal.

(4) The transducer field was computed at increments $\Delta S = 0.1$ with S given in Eq. (5), and the field was numerically integrated over the same area as the transducer by the equivalent of a pressure-and-phase-sensitive transducer as in Ref. 3.

(5) The received signal was converted to dB level and plotted as diffraction loss versus S .

2. Results: Isotropy

The diffraction loss for an isotropic medium, $b = 0$, $A = B = C = D = E = 0$, by the Newberry-Thompson theory using the Gauss-Hermite expansion for a piston source many wavelengths in diameter operated at a single frequency is given in Fig. 3. On this scale, the present theory agrees to within the thickness of the drawn curve (± 0.02 dB) with all previous theories^(1-3, 7-10). In particular, the position S_A of peak A agrees among the theories.

3. Results: Cubic [100] and [111]

Diffraction loss data are available⁽²⁾ for the [100] and [111] directions in several cubic crystals. These had been compared with theory⁽³⁾ by interpolating between loss curves computed at values of b differing by 0.1. Agreement had been found. The expressions for b according to Waterman are as follows:

Cubic [100] Direction

$$b = \frac{(c_{11} - c_{12} - 2c_{44})(c_{11} + c_{12})}{2c_{11}(c_{11} - c_{44})} \quad (15)$$

Cubic [111] Direction

$$b = \frac{2(2c_{44} + c_{12} - c_{11})(c_{11} + 2c_{12} + c_{44})}{3(c_{12} + c_{44})(c_{11} + 2c_{12} + 4c_{44})} \quad (16)$$

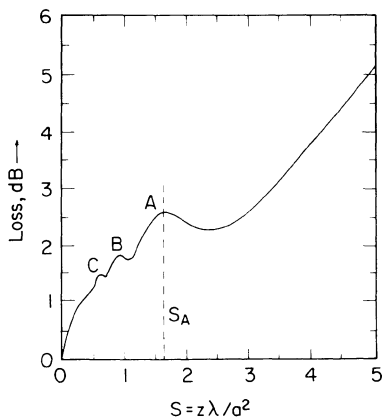


Figure 3 The diffraction loss in an isotropic medium as calculated by the Newberry-Thompson measurement model using the Gauss-Hermite expansion. This curve agrees quantitatively with all previous theories.

These were used in Eq. (7) to find C and E.

Values of the elastic moduli for silicon for which diffraction loss data were available⁽²⁾ were taken from Ref. 11 quoted in Ref. 12. The loss versus S was computed with the Gauss-Hermite model to confirm that the model can indeed handle anisotropic materials. The G-H output is compared with experiment⁽²⁾ in Figs. 4 and 5. The shapes of the curves and the position of Peak A are predicted by the new theory as well as by the previous theory⁽³⁾. The new and previous theories agree exactly, i.e., ± 0.02 dB. The position of Peak A is the most important factor^(1-3,7) in the agreement between theories and experiment.

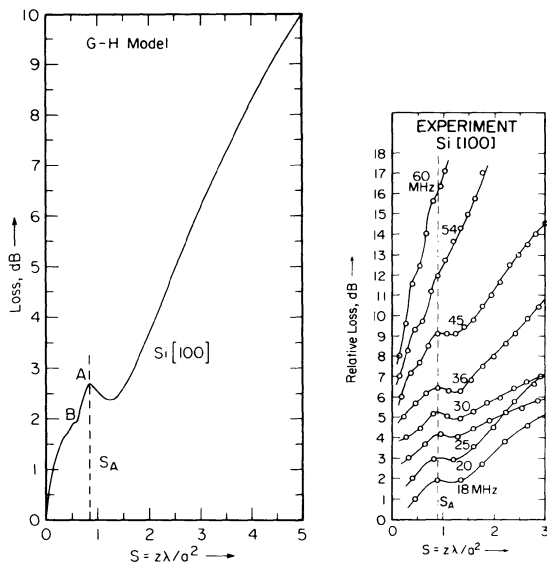


Figure 4 G-H model compared with attenuation experiments for [100] direction in silicon.

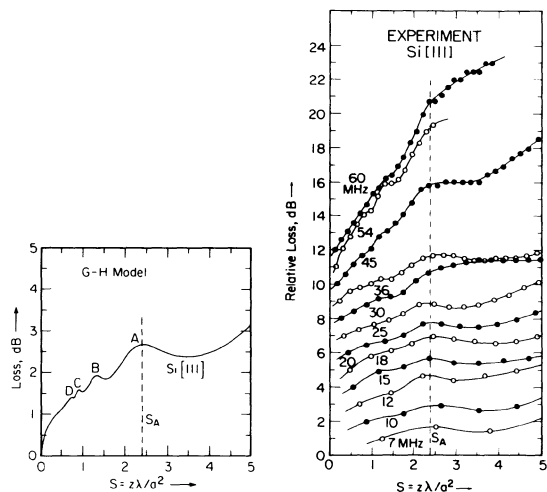


Figure 5 G-H model compared with attenuation experiments for [111] direction in silicon.

From Sections A.2 and 3, we conclude that the Newberry-Thompson theory is verified and can now be used to explain other diffraction loss data previously unexplained.

B. New Results: Cubic [110]

As explained above, [110] cubic data on diffraction loss were not amenable to theoretical explanation previously. Experimental data were published⁽³⁾, however, for Si, Ge, and NaCl. Elastic moduli for these were found in Refs. 11, 13, and 14 within Ref. 12 and used in Eqs. (13) and (14) to provide input for the G-H expansion. The loss curves were computed and are compared with experiment in Figs. 6, 7, and 8.

The theory predicts the general shape of the loss curves and the approximate magnitude. In particular, the experimental shape in which Peak A is only a region of change in slope from steep increasing to a shallow almost-plateau is reproduced by theory. The previous hypothesis⁽³⁾ that the azimuthal variation from positive to negative in the velocity variability for paraxial rays about the [110] direction would result in this plateau behavior has been verified.

CONCLUSIONS

It is concluded that the Gauss-Hermite expansion in the Newberry-Thompson theory can handle saddle points in the slowness surface

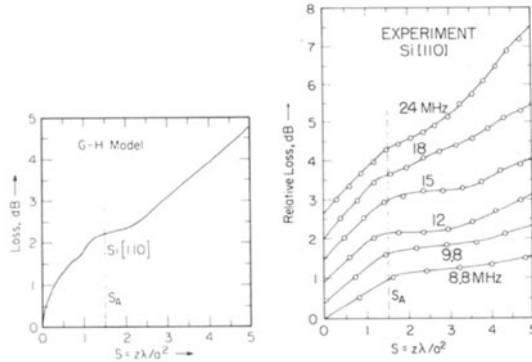


Figure 6 G-H model (Newberry-Thompson theory) used to explain the experimental data on ultrasonic loss in the [110] direction in silicon.

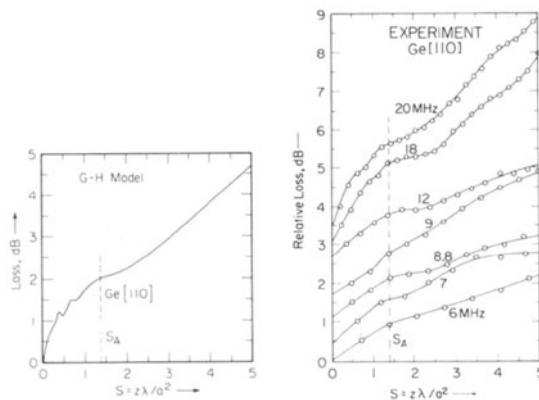


Figure 7 G-H model used to explain the experimental data on ultrasonic loss in the [110] direction in germanium.

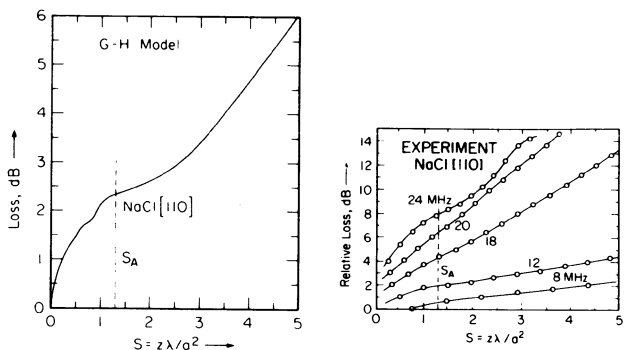


Figure 8 G-H model used to explain the experimental data on ultrasonic loss in the [110] direction in NaCl.

as well as parabolas of revolution. The saddle shape of the slowness surface in the [110] direction in cubic crystals contributes both positive and negative phase increments to the field and accounts for the smoothing out of Peak A in the loss curves. Further work remains to be done on directions of propagation in which none of the coefficients in Eq. (6) are zero.

ACKNOWLEDGMENTS

This work was supported by the Center for NDE at Iowa State University and was performed at the Ames Laboratory. Ames Laboratory is operated for the U.S. Department of Energy by Iowa State University under Contract No. W-7405-ENG-82.

REFERENCES

1. E. P. Papadakis, J. Acoust. Soc. Amer. **35**, 490-494 (1963).
2. E. P. Papadakis, J. Acoust. Soc. Amer. **36**, 414-422 (1964).
3. E. P. Papadakis, J. Acoust. Soc. Amer. **40**, 863-876 (1966).
4. M. J. Lighthill, Philosophical Transactions **A252**, 397-430 (1960).
5. P. C. Waterman, Phys. Rev. **113**, 1240-1253 (1959).
6. B. P. Newberry and R. B. Thompson, J. Acoust. Soc. Amer. **85**, 2290-2300 (1989).
7. H. Seki, A. Granato, and R. Truell, J. Acoust. Soc. Amer. **28**, 230-238 (1956).
8. M. B. Gitis and A. S. Khimunin, Soviet Physics-Acoustics **14**, 305-310 (1969).
9. A. S. Khimunin, Acoustica **27**, 173-181 (1972).
10. G. C. Benson and O. Kiyohara, J. Acoust. Soc. Amer. **55**, 184-185 (1974).
11. H. J. McSkimin and P. Andreatch, Jr., J. Appl. Phys. **35**, 2161-2165 (1964).
12. G. Simmons and H. Wang, Single Crystal Elastic Constants and Calculated Aggregate Properties: a Handbook, The M.I.T. Press, Cambridge, MA, 1971.
13. H. J. McSkimin and P. Andreatch, Jr., J. Appl. Phys. **34**, 651-655 (1963).
14. W. C. Overton and R. T. Swim, Phys. Rev. **84**, 758-762 (1951).